Random error propagation and uncertainty analysis in the dynamic characterization of Tilting Pad Journal Bearings

View the article online for updates and enhancements.

Random error propagation and uncertainty analysis in the dynamic characterization of Tilting Pad Journal Bearings

M Barsanti[1], E Ciulli[1] and P Forte[1]

[1] Department of Civil and Industrial Engineering, University of Pisa, Largo Lazzarino, Pisa, Italy

E-mail: `m.barsanti@ing.unipi.it`, `e.ciulli@ing.unipi.it`, `p.forte@ing.unipi.it`,

Abstract.
   In this work a new statistical method for the determination of the dynamic coefficients of Tilting Pad Journal Bearings is described. The method is applied to the results obtained testing a 5 pads tilting pad journal bearing with 280 mm diameter. Tests were performed on an advanced experimental apparatus specifically realized for investigations on large size high performance bearings for turbomachinery. The linear coefficient identification procedure is based on the dynamic measurement of forces, accelerations and relative displacements of rotor and bearing, as function of excitation frequency for different operating conditions. The post-processing of the dynamic data is performed in the frequency domain using the Fast Fourier Transform. Along with a description of the experimental test and identification procedure, this paper presents a least-square minimization technique for determining the dynamic coefficients and a bootstrap statistical technique for estimating their confidence intervals.

1. Introduction

The characteristics of bearings strongly influence the rotor dynamic behaviour. Therefore the determination of the bearing stiffness and damping coefficients is quite important. This is usually done experimentally, applying dynamic loads to the rotor or to the bearing and measuring their relative displacement. Identification methods are then used to determine the dynamic coefficients, mainly in the frequency domain. In a comprehensive review [1] test apparata and procedures are compared including the methods for evaluating the effects of measurement uncertainty on overall bearing coefficient confidence levels. Most older papers on experimental bearing identification did not include a comprehensive uncertainty analysis and only later its importance was evidenced.

   Indeed an uncertainty analysis is needed in order to validate the experimental results, to increase validity of comparisons of results from different labs or processes, to improve design of experiments and measurement, to provide a reliable tool for quality assurance of measurements and research results [2], last but not least to ease the comparison of experimental and numerical results. In the literature the experimentally determined bearing dynamic coefficients are reported with their uncertainty interval, usually with 95% confidence, referring to the guidelines of ANSI/ASME PTC 19.1 [3] and ISO GUM standards [4]. Very cited is also [5] that describes the sources of errors in engineering measurements, the relationship between error and uncertainty

and the procedure of an uncertainty analysis from the identification of the intended true value of a measurement, the estimation of the individual errors, and results interpretation and reporting. Errors may arise from calibration, data acquisition, and data reduction each with bias (systematic) and precision (random) components [3]. Errors in measurements of various parameters are propagated into derived results through the sensitivity factors that express the relationship between the results and the independent parameters. In the case of journal bearing dynamic coefficients, they are the derived results of measured parameters such as forces, displacements, mass and acceleration. The standards suggest to keep bias and precision errors of the parameters separate until the final result uncertainty computation by two models, sum or RSS.

Though in more recent years papers on experimental journal bearing dynamic characterization include an uncertainty analysis as part of the reported results, few papers give details about the adopted technique to perform such an analysis. Among them, referring to the standards, there are [6, 7] and [8, 9], the latter focusing on systematic errors. In [10] measurement uncertainty propagation in parameter identification of mechanical systems in the frequency domain is dealt with using a multivariate uncertainty analysis.

This paper describes the testing and data processing procedures for the dynamic characterization of a high performance tilting pad journal bearing on an advanced test bench. The test article is statically loaded and excited dynamically with a pseudorandom load, as it has been shown that, due to the short time required to obtain useful data, it reduces the possibility that changes in test conditions will affect identified coefficients, thus reducing uncertainty. The post-processing of the dynamic data is performed in the frequency domain using the Fast Fourier Transform (FFT). The uncertainty associated with random errors in the measurement of relevant parameters in 30 consecutive tests was analyzed statistically using a least-square minimization technique for determining the dynamic coefficients and a bootstrap statistical technique for estimating their confidence intervals.

2. Experimental activity

The experimental apparatus employed in this work was specifically realized for investigations on large size high performance bearings for turbomachinery. The main characteristics of the test rig and the procedure normally used for the identification of the dynamic coefficients are briefly described below.

The test rig, described in more detail in [11, 12, 13], is shown in figure 1. Bearings with diameters from 150 mm to 300 mm and bearing length to diameter ratio from 0.4 to 1 can be tested. A configuration with a floating test bearing housing at the centre of a rotor supported by two rolling bearings is adopted.

The rotor is driven by a 630 kW electric motor connected to a multiplier with a transmission ratio of 6 so that the shaft maximum rotational speed is 24000 rpm. Static and dynamic loads are applied to the bearing case by three hydraulic actuators, Figure 2. The static actuator is able to apply a maximum load of 270 kN upwards, while the dynamic actuators are able to apply up to 40 kN loads, each one at 45° with respect to the vertical direction. The dynamic load is obtained from the sum of up to five sinusoidal excitations (tones) individually adjustable in terms of amplitude and frequency up to a maximum dynamic frequency of 350 Hz. The dynamic actuators can work one at a time or simultaneously, in the latter case producing a vertical force when operating with equal amplitude in phase, and a horizontal force when in antiphase. A load cell with 300 kN full-scale is located between the static actuator and the bearing case. Two instrumented stingers, located between the dynamic actuators and the case, act as triaxial load cells, with 40 kN full-scale, for measuring dynamically all significant force components.

The bearing oil flow rate can be varied from 125 to 1100 l/min and the oil inlet temperature from 30 to 120 °C. The plant maximum total required power is 1000 kW. Eight proximity sensors,
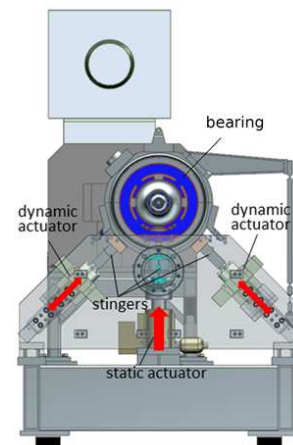
Figure 1. Picture of the test rig.

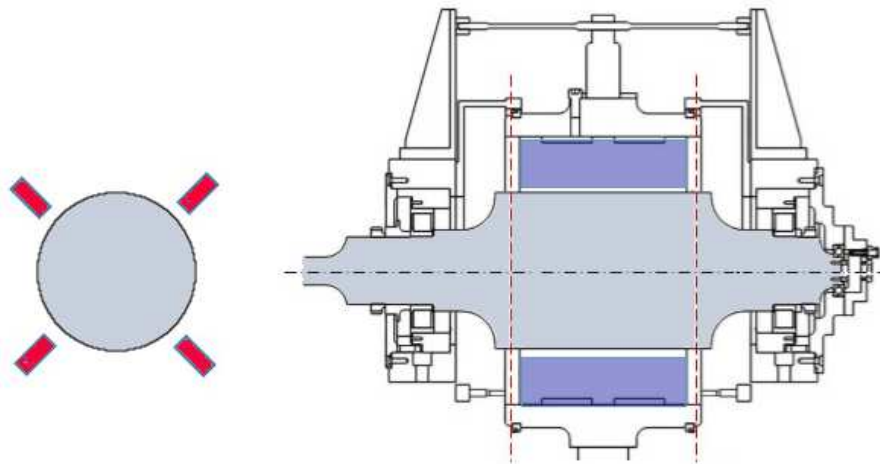**Figure 2.** Load application systems.

Figure 3. Schematic drawing showing the position of the proximity sensors (red rectangles). The red dashed lines indicate the sensor planes.

with a sensitivity of about 0.1 μm and a measuring range of 2000 μm, are placed on two parallel planes perpendicular to the bearing axis for measuring the relative displacements of the bearing housing and the rotor along the directions of the dynamic actuators (see Fig. 3). Accelerometers are employed to measure the stator acceleration at the mid-section, in the direction of the dynamic actuators. Tests are managed by a very complex control and data acquisition system. About 30 high-frequency signals are usually sampled at 50 kHz while about 60 low-frequency signals are sampled at 1 Hz.

3. Identification procedure for the dynamic coefficients

The dynamic stiffness and damping coefficients are evaluated from the data recorded during two tests with linearly independent excitations for each excitation frequency. In-phase and anti-phase operation modes of the dynamic actuators are used for obtaining the two necessary sets of data. The FFT of the signals is used for the identification process of the dynamic coefficients. Single-tone and multi-tone test can be performed. The use of the FFT allows the extraction of forces, displacements and accelerations components at single frequencies also in the multi-tone

test. For each excitation frequency the following calculation procedure is followed. First the net bearing film force is determined by subtracting the stator inertia from the measured forces applied to the stator:

$$\left[\begin{array}{cc} F_{b1x} & F_{b2x} \\ F_{b1y} & F_{b2y} \end{array}\right] = \left[\begin{array}{cc} F_{s1x} & F_{s2x} \\ F_{s1y} & F_{s2y} \end{array}\right] - M\left[\begin{array}{cc} A_{1x} & A_{2x} \\ A_{1y} & A_{2y} \end{array}\right] \tag{1}$$

where F indicates the amplitude of the force transform, A the amplitude of the acceleration transform, M the stator mass, while for the subscripts b and s refer to bearing and stator respectively, x and y refer to the horizontal and vertical direction respectively, 1 and 2 to the in-phase and anti-phase test respectively.

According to the classical linear model the net bearing film forces can be related to the corresponding displacements by the so called bearing impedance matrix H.

$$\left[\begin{array}{cc} F_{b1x} & F_{b2x} \\ F_{b1y} & F_{b2y} \end{array}\right] = \left[\begin{array}{cc} H_{xx} & H_{xy} \\ H_{yx} & H_{yy} \end{array}\right]\left[\begin{array}{cc} X_1 & X_2 \\ Y_1 & Y_2 \end{array}\right] \tag{2}$$

where H_{ij} are the (complex) elements of the impedance matrix. Then H is determined, in the frequency domain, using the classical methodology described in [14], simply by multiplying the [2×2] force complex matrix by the corresponding inverse displacement complex matrix:

$$\left[\begin{array}{cc} H_{xx} & H_{xy} \\ H_{yx} & H_{yy} \end{array}\right] = \left[\begin{array}{cc} F_{b1x} & F_{b2x} \\ F_{b1y} & F_{b2y} \end{array}\right]\left[\begin{array}{cc} X_1 & X_2 \\ Y_1 & Y_2 \end{array}\right]^{-1} \tag{3}$$

where X, Y indicate the amplitudes of the displacement transform for in-phase (subscript 1) and anti-phase (subscript 2) tests. The stiffness k and damping c coefficients are finally obtained as respectively the real and the imaginary parts of the impedance direct and cross-coupled coefficients.

$$\left[\begin{array}{cc} H_{xx} & H_{xy} \\ H_{yx} & H_{yy} \end{array}\right] = \left[\begin{array}{cc} k_{xx} & k_{xy} \\ k_{yx} & k_{yy} \end{array}\right] + i\omega\left[\begin{array}{cc} c_{xx} & c_{xy} \\ c_{yx} & c_{yy} \end{array}\right] \tag{4}$$

Once the coefficients are calculated at all the excitation frequencies, interpolation at the rotational frequency yields the synchronous dynamic coefficients. For each operating condition, 30 samples of forces and displacements are available, each obtained by FFT on a 3 s time window. The dynamic coefficients are usually computed averaging a sample of impedance matrices obtained in the same operating conditions.

In this work different techniques are proposed for both the determination of the mean impedance matrix and the evaluation of the random errors on the estimated mean values. Focusing on random errors, the systematic uncertainty is not considered here, the experimental apparatus is assumed to be perfectly calibrated and other parameters needed to build the data set, such as the mass M, are considered to be exactly known.

4. Statistical model
Adopting the linear model of equation (2) the (complex) elements of the impedance matrix can be computed from the experimental data, assuming that at every variation of the position matrix corresponds a variation of the force matrix. For computing purposes, eq. (2) is expressed separating the real and the imaginary part of all the complex quantities, obtaining relationships

among real quantities:

$$
\begin{cases}
\text{Re}(F_{b1x}) = k_{xx}\text{Re}(X_1) - \omega c_{xx}\text{Im}(X_1) - \omega c_{xy}\text{Im}(Y_1) + k_{xy}\text{Re}(Y_1) \\
\text{Im}(F_{b1x}) = k_{xx}\text{Im}(X_1) + k_{xy}\text{Im}(Y_1) + \omega c_{xx}\text{Re}(X_1) + \omega c_{xy}\text{Re}(Y_1) \\
\text{Re}(F_{b2x}) = k_{xx}\text{Re}(X_2) - \omega c_{xx}\text{Im}(X_2) - \omega c_{xy}\text{Im}(Y_2) + k_{xy}\text{Re}(Y_2) \\
\text{Im}(F_{b2x}) = k_{xx}\text{Im}(X_2) + k_{xy}\text{Im}(Y_2) + \omega c_{xx}\text{Re}(X_2) + \omega c_{xy}\text{Re}(Y_2) \\
\text{Re}(F_{b1y}) = k_{yx}\text{Re}(X_1) - \omega c_{yx}\text{Im}(X_1) - \omega c_{yy}\text{Im}(Y_1) + k_{yy}\text{Re}(Y_1) \\
\text{Im}(F_{b1y}) = k_{yx}\text{Im}(X_1) + k_{yy}\text{Im}(Y_1) + \omega c_{yx}\text{Re}(X_1) + \omega c_{yy}\text{Re}(Y_1) \\
\text{Re}(F_{b2y}) = k_{yx}\text{Re}(X_2) - \omega c_{yx}\text{Im}(X_2) - \omega c_{yy}\text{Im}(Y_2) + k_{yy}\text{Re}(Y_2) \\
\text{Im}(F_{b2y}) = k_{yx}\text{Im}(X_2) + k_{yy}\text{Im}(Y_2) + \omega c_{yx}\text{Re}(X_2) + \omega c_{yy}\text{Re}(Y_2)
\end{cases}
\tag{5}
$$

In a real experiment, the presence of noise (random error) causes the relationships shown in eq. 5 to be not exactly verified. This model, which describes the mechanical behavior of the system, does not take into account other factors that will introduce uncertainty in each measured value, and which cannot be taken into account in such a simple model. Therefore we introduce an uncertainty (random variable) added to the "true" values of each of the real variables. The uncertainties are modeled as zero mean Gaussian additive noises. Their standard deviations depends on the precision of the sensors of displacement and force, and on the short-term stability of the experimental conditions. Section 5 will show the importance of the estimation of the standard deviation in the implementation of the statistical technique for the computation of the dynamic coefficients.

5. Fit technique
It is possible to estimate the "best" values (the best approximations to the "true" values) of FFT amplitudes of bearing forces and relative displacements together with the estimates of the elements of the impedance matrix. This is obtained introducing the best estimates of forces, displacements and impedance matrix elements (indicated with a hat sign) and assuming that the relationships shown in eq. 5 are exactly verified for the best estimates. In order to obtain the best estimates of all the quantities, a constrained minimum of the following weighted sum of squared residuals S as a function of the dynamic coefficients, displacements and forces is searched:

$$
\begin{aligned}
S = \sum_{i=1}^{N} \Bigg[& \left|\frac{\hat{X}_{1,i} - X_{1,i}}{\sigma_X}\right|^2 + \left|\frac{\hat{X}_{2,i} - X_{2,i}}{\sigma_X}\right|^2 + \left|\frac{\hat{Y}_{1,i} - Y_{1,i}}{\sigma_Y}\right|^2 + \left|\frac{\hat{Y}_{2,i} - Y_{2,i}}{\sigma_Y}\right|^2 + \\
& \left|\frac{\hat{F}_{b1x,i} - F_{b1x,i}}{\sigma_{Fx}}\right|^2 + \left|\frac{\hat{F}_{b2x,i} - F_{b2x,i}}{\sigma_{Fx}}\right|^2 + \left|\frac{\hat{F}_{b1y,i} - F_{b1y,i}}{\sigma_{Fy}}\right|^2 + \left|\frac{\hat{F}_{b2y,i} - F_{b2y,i}}{\sigma_{Fy}}\right|^2 \Bigg]
\end{aligned}
\tag{6}
$$

in which the relationships (among the hat variables) shown in equation (5) are the constraints. Note that the standard deviations are assumed to have the same value for all the displacements and for all the forces. This is the easiest assumption, and its validity will be shown in section 6 together with the estimation of σ_X and σ_F from the available data.

6. Method for the estimate of standard deviations
The starting point for the estimate of the standard deviations σ_X and σ_F, that are the weights in equation (6), is the analysis of the dispersion of the acquired data. As the bench control system acts for the stabilization of the force intensities (regardless of their phases), the distribution of the moduli $|X_1|$, $|Y_1|$, $|X_2|$, $|Y_2|$, $|F_{b1x}|$, $|F_{b1y}|$, $|F_{b2x}|$, $|F_{b2y}|$ has been carried out. The standard deviations of the empirical distributions of the moduli of the displacements and of the forces are plotted in Figure 4 (a) and (b) respectively as a function of the ratio between excitation frequency and shaft rotation frequency, for two different shaft rotational frequencies.

It is possible to notice that the standard deviations strongly depend on both excitation frequency and shaft rotational frequency. An analysis of equation (6) evidences, however, that
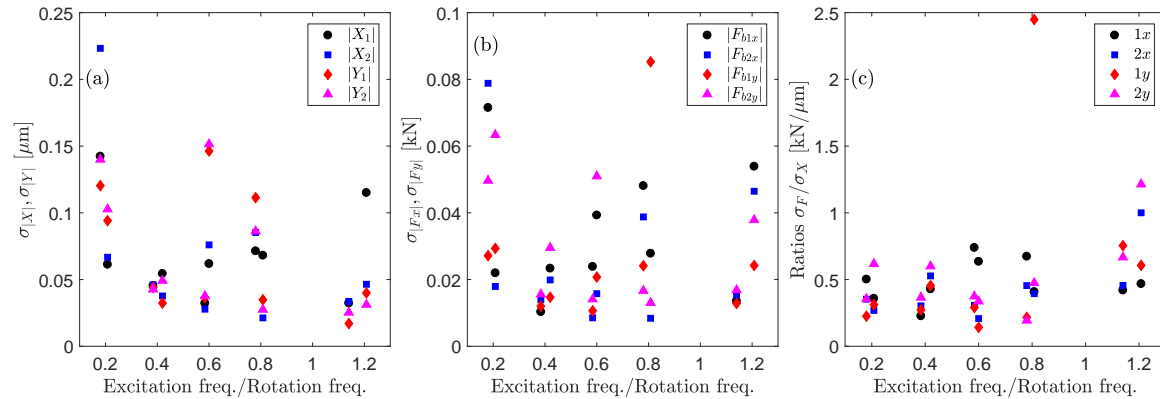
Figure 4. Standard deviations of the empirical distributions of the moduli of displacements and forces. (a): displacements, (b): forces (c): ratios between standard deviations.

the values of the hat variables at which the minimum S is obtained remains unchanged if σ_X and σ_F are modified keeping their ratio constant. Therefore, an analysis of the ratios σ_F/σ_X has been carried out in order to estimate the relative precision of the two measurements, and the results are shown in Figure 4 (c). It seems evident that the large majority of the ratios lies in the interval between 0.2 and 0.8 kN/μm, therefore a choice of $\dfrac{\sigma_F}{\sigma_X} = 0.5\dfrac{\text{kN}}{\mu\text{m}}$ seems to be reasonable. Considering the sensitivities of the displacement and force sensors, as reported in the respective data sheets, $\sigma_{|X|} = \sigma_{|Y|} = 0.1\mu$m was set for all the displacement measurements and $\sigma_{|F_x|} = \sigma_{|F_y|} = 50\,$N for all the force measurements.

7. Best fit estimation of dynamic coefficients
The reported results were obtained testing a 45 kN load acting on a tilting pad journal bearing with a diameter of 280 mm with 5 pads in load-between-pad configuration. Two cases at low (2000 rpm) and high (7500 rpm) rotating speed were analyzed. The experimentally obtained values of the stiffness and damping coefficients fall within the ranges predicted by the bearing manufacturer using a proprietary code based on thermo-elastic hydrodynamic lubrication models, taking into account many factors affecting the bearing performance (e.g. geometric tolerances, temperature effects, presence of turbulence).

The minimization procedure of quantity S defined in equation (6) was carried out using R software [16], and taking as starting point the values of dynamic coefficients computed using equation 3 and of the measured displacements. Usually the relative difference between the results obtained with best fit technique and the ones obtained by averaging the impedance matrices computed using equation 3 is lower than 1%. In some cases higher discrepancies are obtained in the estimation of some of the cross-coupled damping coefficients, and this difference is probably due to the fact that the estimate of very small damping parameters is very difficult. The results for 5 different excitation frequencies at two different shaft rotating frequencies (2000 rpm and 7500 rpm) are shown in Figure 5.

A first advantage of this computational method is that it includes the best estimates of not only the dynamic coefficients but of forces and displacements as well, making it possible to check if their discrepancies with respect to the measured values are in agreement with the sensors precision. An example of this result is shown in Figure 6.

A second advantage is that the linear model can be easily extended to more complex ones. Zero-checking and nonlinearities can be easily added inserting a constant or higher degree terms in equation 2. It is possible to develop more complex models in which some relationships between
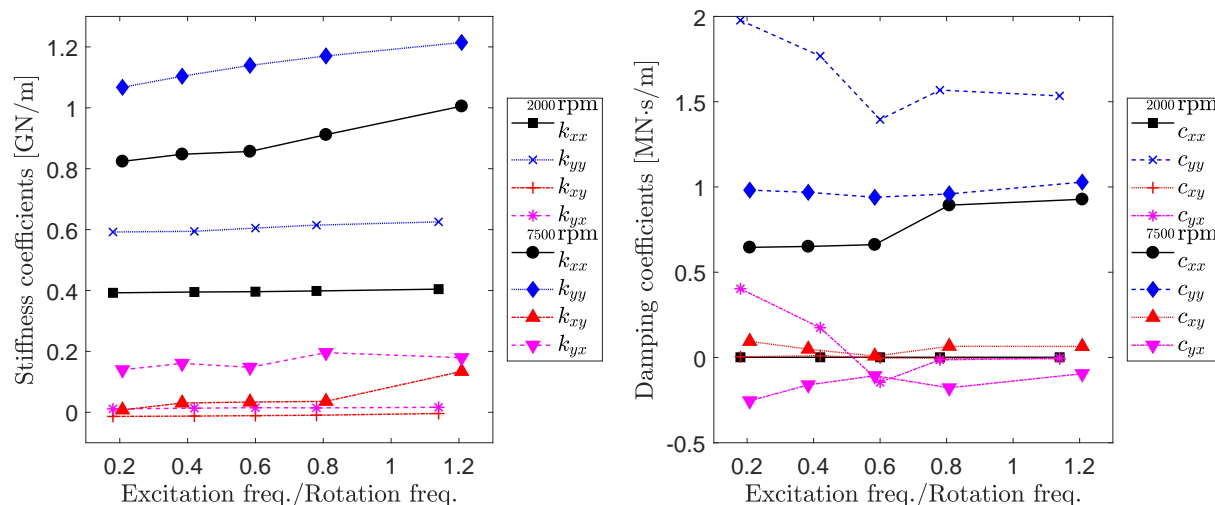
Figure 5. Dynamic coefficients as a function of the relative excitation frequency.
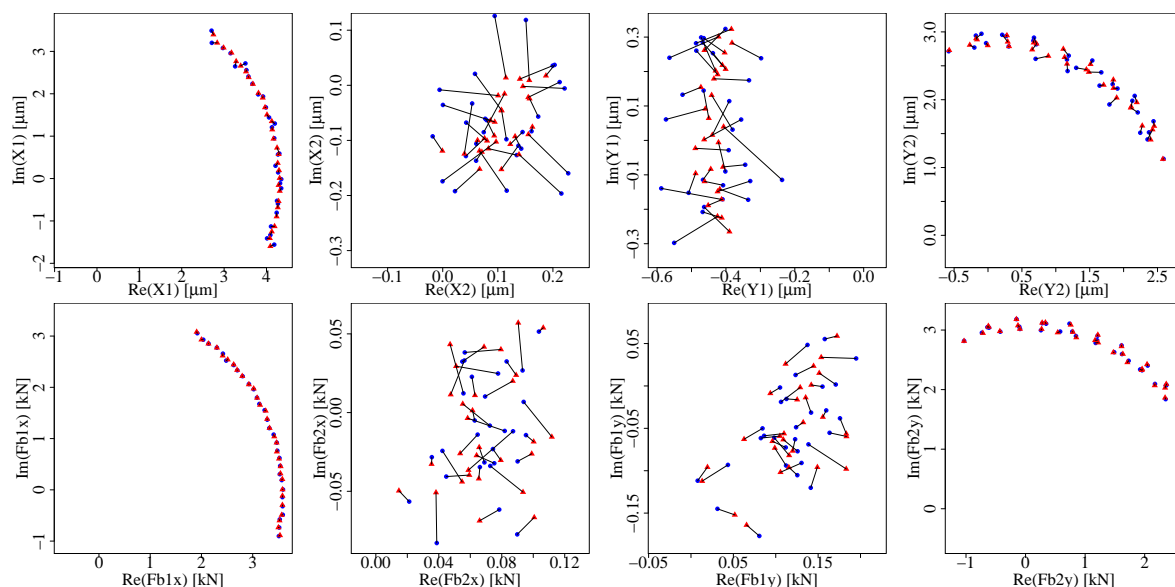

Figure 6. An example of measurement of displacements and forces. In the complex plane, blue circles are measurements and red triangles are the corresponding values estimated with the fitting procedure. Note that scales on axes are different for each panel.

the elements of the impedance matrix and the dynamic coefficients are hypothesised, and data acquired in different operating conditions are fitted all together in a single model. The next section will show that the most important improvement produced by this method consists in estimating the random uncertainties due to fluctuations in the measurements.

8. Bootstrap random uncertainty estimation
The boostrap is a standard statistical technique [15] used to estimate the distribution of a random quantity and for the computation of the associated confidence intervals. The main advantage of this method is that it is not dependent on the distribution of the population (therefore its knowledge is not necessary, contrary to what happens for Monte Carlo technique).
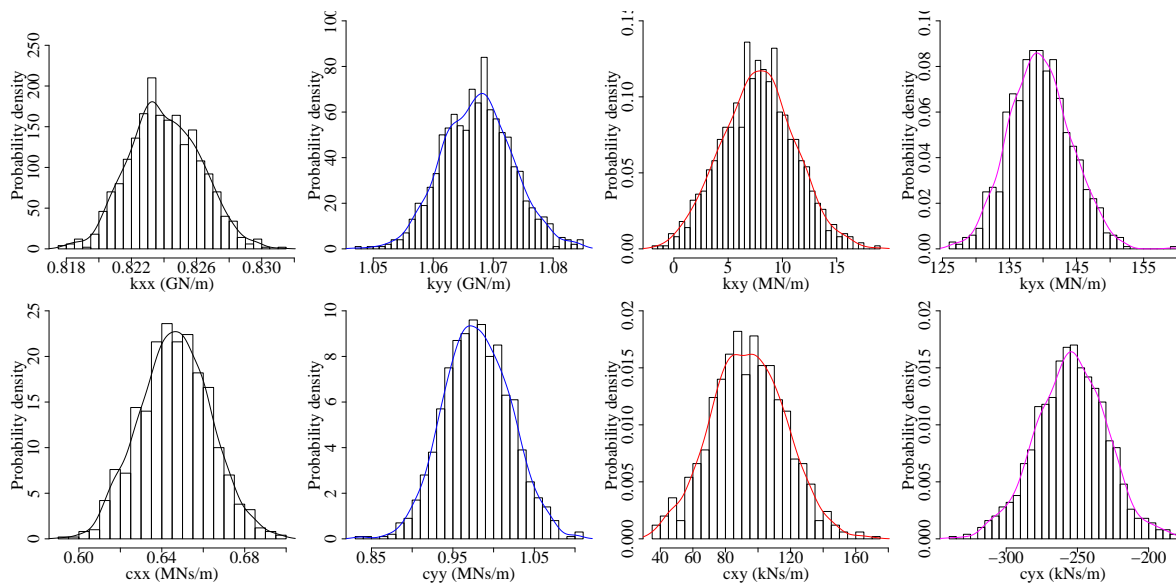
Figure 7. Example of bootstrap distribution for the dynamic coefficients obtained for a rotation speed of 7500 rpm and an excitation frequency of 26 Hz. The superimposed continuous curves are analytical estimates of the distribution functions obtained using kernel method, reported only to show that lack of Gaussianity is evident in many cases.

Bootstrapped confidence intervals can be derived for any numerical statistic based on a random sample. Moreover, it can be used with samples containing only few data. The bootstrap algorithm works by drawing B independent bootstrap samples extracting them from the original dataset (drawing with replacement). In this work, $B = 1000$ is used. For each extraction, the minimization of S (equation 6) is carried out, therefore obtaining a set $H_{ij}^{(k)}$ of parameters of the linear model, with $k = 1, \ldots, B$. At the end of this procedure, a bootstrap distribution of the parameters is obtained, that is statistically equivalent to the distribution that would have been obtained by repeating the experiment B times. An example of this result is shown in Figure 7.

From the boostrap distribution, any empirical quantile can be extracted, if B is big enough. In order to obtain the extremes of a 95% confidence interval, the results of the B fittings for each dynamic coefficient are sorted in ascending order, and the values at the 25th and 975th positions are the lowest and highest estremes respectively. These confidence intervals can be plotted as error bars for each experimental condition. The results (already shown all together in Figure 5) are shown in Figure 8 for stiffness coefficients and in Figure 9 for damping coefficients together with the respective estimated 95% confidence intervals.

A large variety of confidence intervals width is evident. Some values of the dynamic coefficients have a very high precision, other ones are much more dispersed. In some cases the dispersion is comparable to the variation with the excitation frequency of the dynamic coefficient itself. That is the case of cross-coupled stiffness, k_{yx}, and damping coefficients for some particular frequency and rotational speed. In other cases the precision is sufficient to highlight a dependence of the dynamic coefficient on the excitation frequency.

9. Conclusions
This paper presented a statistical method for the determination of dynamic coefficients of a Tilting Pad Journal Bearing. The algorithm computes both the best estimate of their mean value and of their 95% confidence intervals using least square weighted minimization and bootstrap
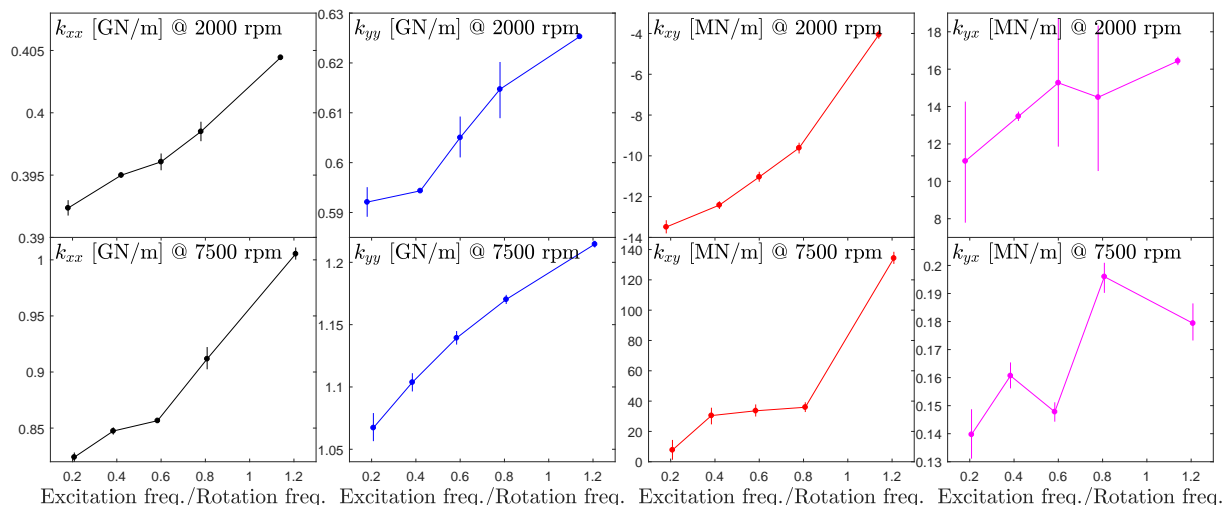
Figure 8. Stiffness coefficients as a function of the relative excitation frequency for two different shaft rotational speeds. Note that the scales are different in each panel to highlight the different amplitudes of the confidence intervals.

Figure 9. Damping coefficients as a function of the relative excitation frequency for two different shaft rotational speeds. Note that the scales are different in each panel to highlight the different amplitudes of the confidence intervals.
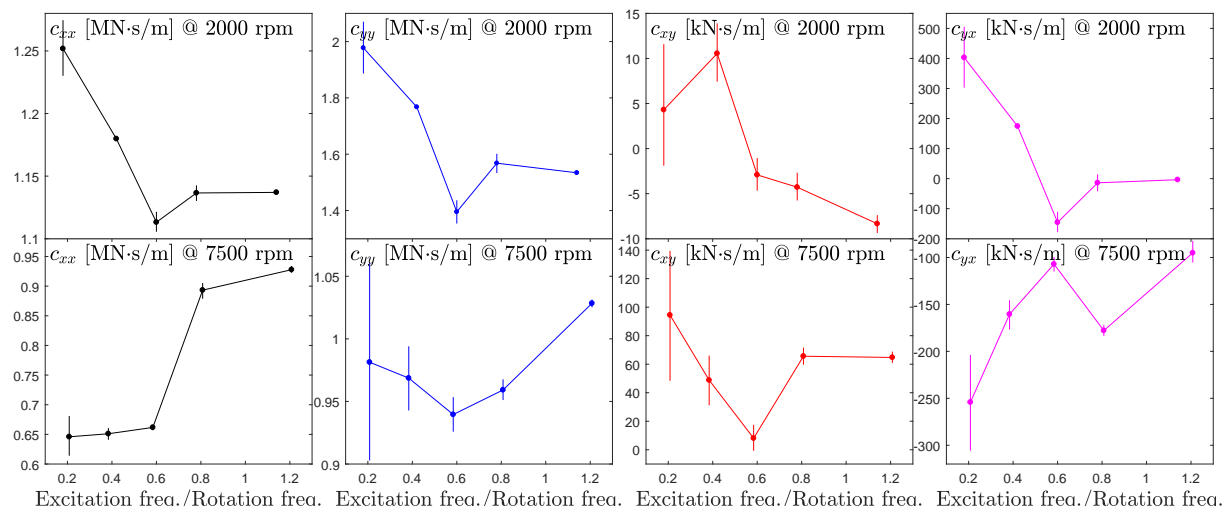
resampling for the estimate of the probability distributions.

The most significant result of this work is that the random uncertainties associated to each stiffness or damping coefficient are obtained, without assuming any hypothesis of gaussianity either on the sample or on the estimated mean values. A large variety of confidence intervals width was found in the processed results. Some values of the dynamic coefficients have a very high precision, other ones are much more dispersed at particular frequencies. Such dispersion will be object of further investigation. In most cases the precision is sufficient to highlight a dependance of the dynamic coefficient on the excitation frequency. The systematic uncertainty was not taken into consideration in this work. A future development will include the study the accuracy of the dynamic coefficients estimates, taking into account the influence of the calibration

technique and of some other external parameters on the estimate of the mean value, and the variation caused by them will be compared with the random uncertainty due to fluctuations in the measurements themselves.

References

[1] Dimond T W, Sheth P N, Allaire P E and He M 2009 Identification methods and test results for tilting pad and fixed geometry journal bearing dynamic coefficients – A review *Shock and Vibration* **16** 13–43

[2] Wells C V 1992 Principles and applications of measurement uncertainty analysis in research and calibration *3rd Ann. infrared radiometric sensor calibration symp.* September 14-17 Logan Utah (USA)

[3] ANSI/ASME PTC-19.1 2013 *Test uncertainty* (New York: ASME)

[4] ISO/IEC Guide 98-3 2008 *Guide to the expression of uncertainty in measurement* (Geneva: ISO)

[5] Moffat R 1988 Describing the uncertainties in experimental results *Exp. Thermal and Fluid Sci.* **1** 3–17

[6] Kostrzewsky G J and Flack R D 1990 Accuracy evaluation of experimentally derived dynamic coefficients of fluid film bearings Part I. Development of method *Tribol. Trans* **33** 105–14

[7] Childs D and Hale K 1994 A test apparatus and facility to identify the rotordynamic coefficients of high-speed hydrostatic bearings *J. Tribol.* **116** 337–44

[8] Dmochowski W 2008 Experimental and theoretical investigations of the dynamic properties for tilting-pad journal bearings *Australian J. of Mech. Eng.* **6** 9–14

[9] Salazar J G and Santos I F 2016 Experimental identification of dynamic coefficients of lightly loaded tilting-pad bearings under several lubrication regimes *Proc. Inst. of Mech. Eng. Part J: J. Eng. Trib.* **230** 1423–38

[10] Medina L U, Diaz S E and LLatas I, 2010 Measurement uncertainty propagation in parameter identification of mechanical systems in frequency domain *Proc. Int. Conf. on Noise and Vibration Eng.* September 20-22 Leuven (Belgium) 5129–41

[11] Forte P, Ciulli E and Saba D 2016 A novel test rig for the dynamic characterization of large size tilting pad journal bearings *J. Phys.: Conf. Series* **744** 012159

[12] Forte P, Ciulli E, Maestrale F, Nuti M and Libraschi M 2018 Commissioning of a novel test apparatus for the identification of the dynamic coefficients of large tilting pad journal bearings *Procedia Structural Integrity* **8** 462–73

[13] Ciulli E, Forte P Libraschi M and Nuti M 2018 Set-up of a novel test plant for high power turbomachinery tilting pad journal bearings *Trib. Int.* **127** 276–87

[14] Al-Ghasem A and Childs D 2005 Rotordynamic coefficients measurements versus predictions for a high-speed flexure pivot tilting pad bearing (load-between-pad configuration) *ASME Turbo Expo 2005: power for land, sea, and air* June 6-9 Reno Nevada (USA) vol 4 p 725–36

[15] Efron B and Tibshirani R J 1993 *An introduction to the bootstrap* (London: Chapman and Hall)

[16] R Development Core Team 2008 *R: A language and environment for statistical computing* (Wien: R Foundation for Statistical Computing)